ADMINISTRATION OF THE DRUG TO EFFECTIVELY KILL THE CANCER CELLS ONLY, WITHOUT DAMAGING THE HEALTHY CELLS, IN EFFECTIVE COST USING NANOBOTS

[1,4]*Nirnimesh De, [2,4]Souhardya Roy and [3,4]Subham Ghosal

[1]Department of Mechanical Engineering, Jadavpur University, Kolkata-700032, India.
[2]Department of Medicine and Surgery, IQ City Medical College, Durgapur-713206, India.
[3]Department of Electrical Engineering, Techno India University, Salt Lake, Kolkata-700091, India.
[4]Jagadis Bose National Science Talent Search Senior Scholar 2018.

*Corresponding Author: Nirnimesh De

Department of Mechanical Engineering, Jadavpur University, Kolkata-700032, India.

ABSTRACT

Drugs that target microtubules are thought to inhibit cell division and cell migration by suppressing dynamic instability, a "**Search & Capture**" behavior that allows microtubules to probe their environment. Here, we report that subtoxic drug concentrations are sufficient to inhibit plus-end microtubule dynamic instability and cell migration without affecting cell division or microtubule assembly. The higher drug concentrations needed to inhibit cell division act through a novel mechanism that generates microtubule fragments by stimulating microtubule minus-end detachment from their organizing centers. The frequency of microtubule detachment in untreated cells increases at prophase suggesting that it is a regulated cellular process important for spindle assembly and function. We observed that drugs produce differential dose-dependent effects at microtubule plus and minus-ends to inhibit different microtubule-mediated functions. This is the basic mechanism of an anti-cancer drug. We are using different techniques to identify the mutated genes as well as 3D protein structure analysis for Mutation Data scoring and Hotspot founding for cancer analysis. We have introduced several markers for this identification process. By this suitable identification, the novelty of the approach comes with the use of the Nanorobots (Nanobots or Nanoids) i.e. typically devices ranging in size from 0.1-10 μm and constructed of Nanoscale or molecular components. As non artificial non-biological Nanorobots have so far been created, they remain a hypothetical concept at this time. Nanobots and its uses Nanobots are robots that carry out a very Specific function and are 50-100 nm Wide. They can be used very effectively for drug delivery. Normally, drugs work through the entire body before they can reach the disease-affected area. Using Nanotechnology, the drug can be Targeted to a precise location which would make the drug much more Effective and reduce the chances of Possible side effects. A great advantage of using Nanobots for drug delivery is that the amount and time of drug release can be easily controlled by controlling the electrical pulse. Furthermore, the walls dissolve easily and are therefore harmless to the body. Description of all the process as well as the mechanisms are explained in this paper.

Graphical Abstract
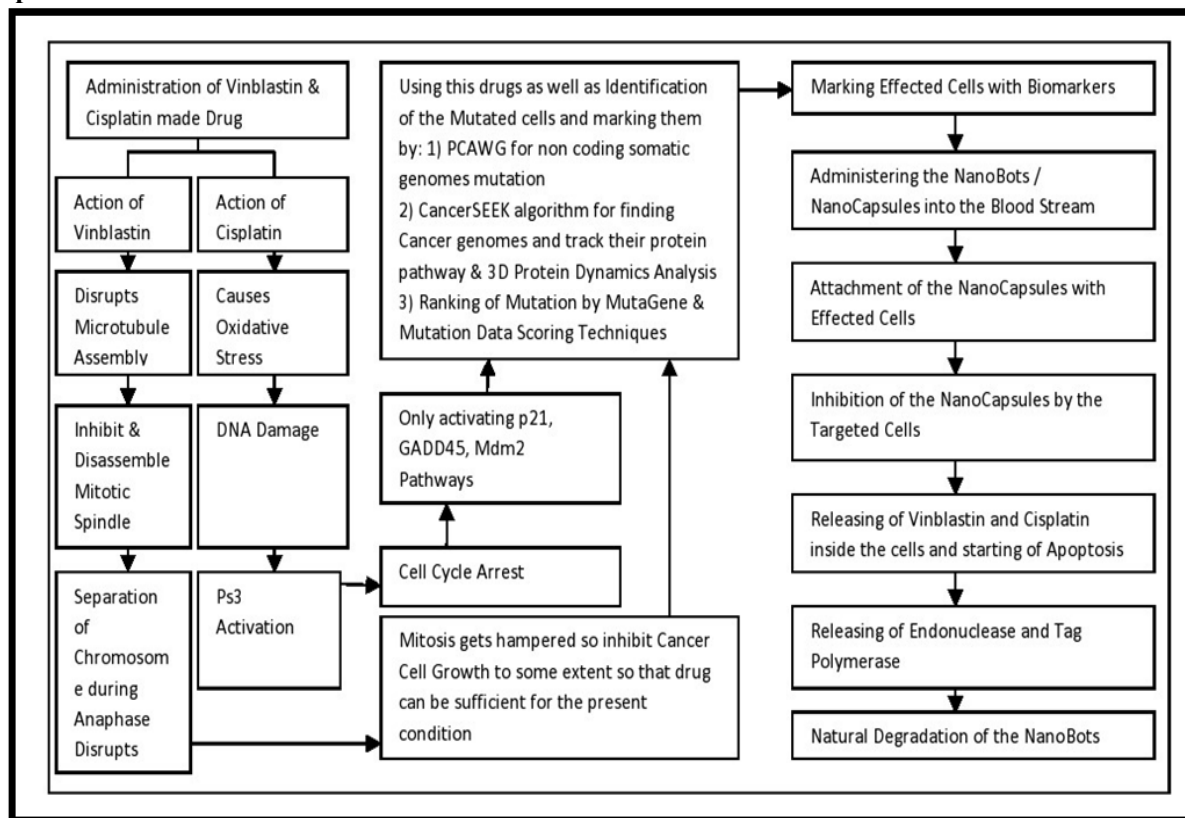
INTRODUCTION

Microtubules are essential cytoskeletal structures that have been implicated in many important cellular processes including vesicle transport, cell structure and motility, signaling, and cell division. They appear as small hollow tubes whose walls are composed of Protofilaments assembled from the head-to-tail addition of **αβ-tubulin heterodimers**. This ordered assembly generates polar microtubules that are arranged with their minus-ends embedded in nucleating centers, called centrosomes, located near the nuclear membrane, and with their plus-ends extended out toward the cell periphery. Microtubules are highly dynamic filaments that exhibit a behavior called dynamic instability. Microtubules engaged in dynamic instability experience stochastic episodes of growth and shortening of their plus-ends interspersed with variable periods of pause during which there is no net change in length .As microtubules are essential for assembly and functioning of the mitotic spindle apparatus, drugs that bind tubulin inhibit chromosome segregation and block cell division. These toxic effects have led to the widespread use of these agents in the treatment of cancer. For example, the microtubule inhibitors (MIs) **Vinblastine and Vincristine** have been used since the 1960s and remain first line drugs for the treatment of lymphoma, leukemia, and testicular carcinoma. More recently, taxanes such as Paclitaxel have been shown to be very effective against breast and ovarian carcinoma, non-small cell lung carcinoma, head and neck tumors, Kaposi's sarcoma, and others. Although all of these drugs are effective in blocking cell division, they have differing effects on microtubule assembly. One group of MIs that includes vinca alkaloids, colchicine, and colcemid disrupts assembly and causes a depletion of cellular microtubules. A second group that includes Taxanes and Epothilones promotes assembly and causes increased microtubule density and bundling in treated cells. Despite these differences, both groups of drugs inhibit the normal progression of cells through mitosis.

EXPERIMERNTAL OBSERVATIONS
PHARMACOLOGICAL ASPECT OF DRUGS IN CANCER CELL GROWTH REDUCTION AND ITS VARIOUS MECHANISMS

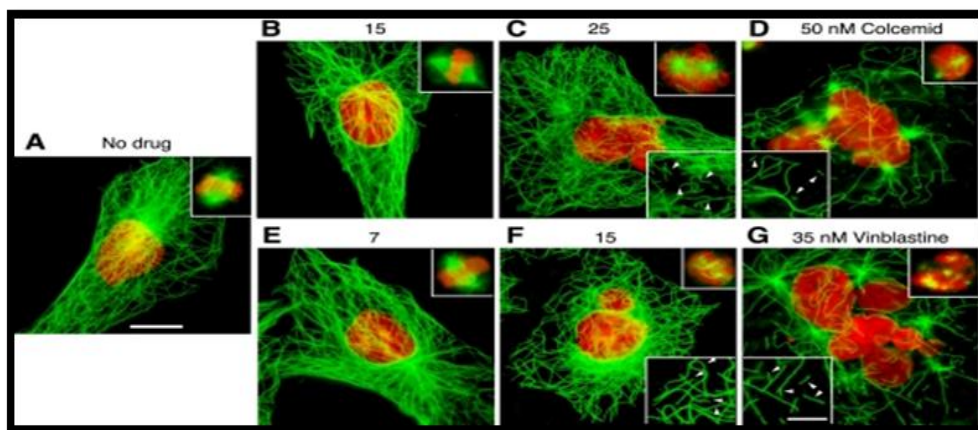- ON Chinese hamster ovary (CHO), CHO mutants CV 2-8, Tax 5-6

Figure 1: Tubulin Immunofluorescence: CHO cells were treated for 2 days with the indicated concentrations of colcemid or vinblastine and stained with DM1A for tubulin (*green*) and DAPI for DNA (*red*). *Bar* = 10 µm. *Upper insets* show representative mitotic cells at each of the indicated drug concentrations. *Lower insets* show 1.5-fold enlargements of a part of the cell to more clearly indicate the presence of microtubule fragments (*arrowheads*); *bar* = 5 µm.
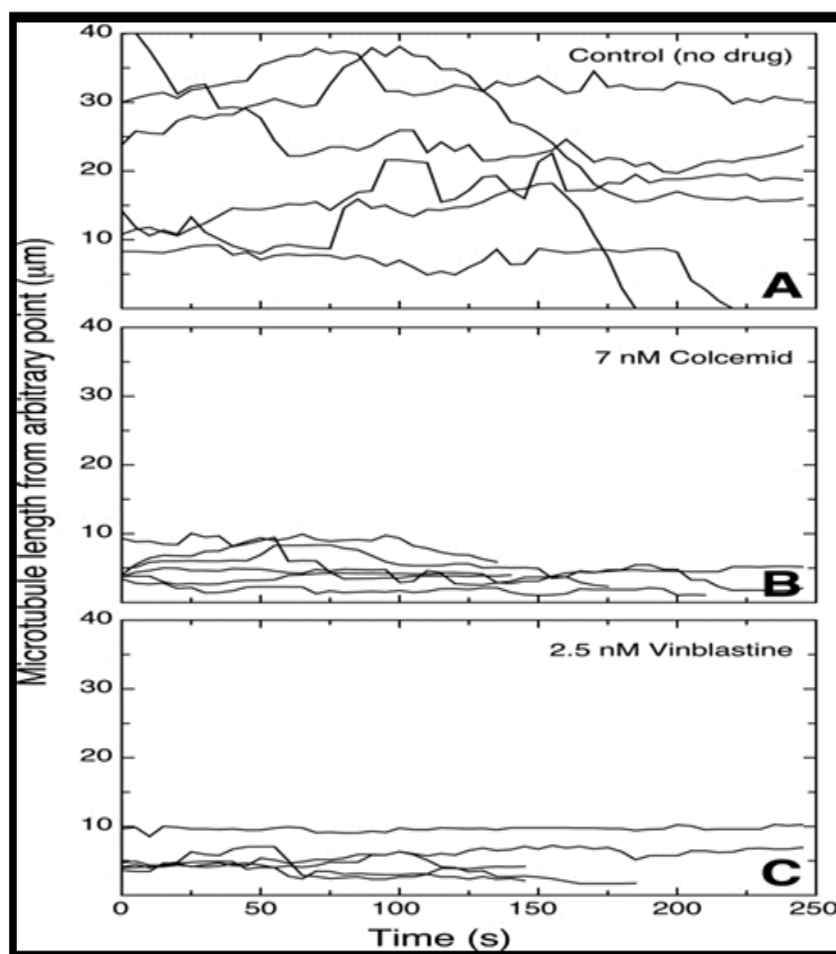

Figure 2: Microtubule Life History Ploting: CHO cells were transfected with EGFP-MAP4, grown overnight, and examined by time-lapse fluorescence microscopy at 37 °C 30 min after the addition of Colcemid or Vinblastine. Images were taken every 5 seconds, and the microtubule length, measured from an arbitrary fixed point, was plotted against time. Each *line* represents a different microtubule. The drug concentrations were chosen to suppress microtubule dynamics without affecting cell division as much as possible (maximum).
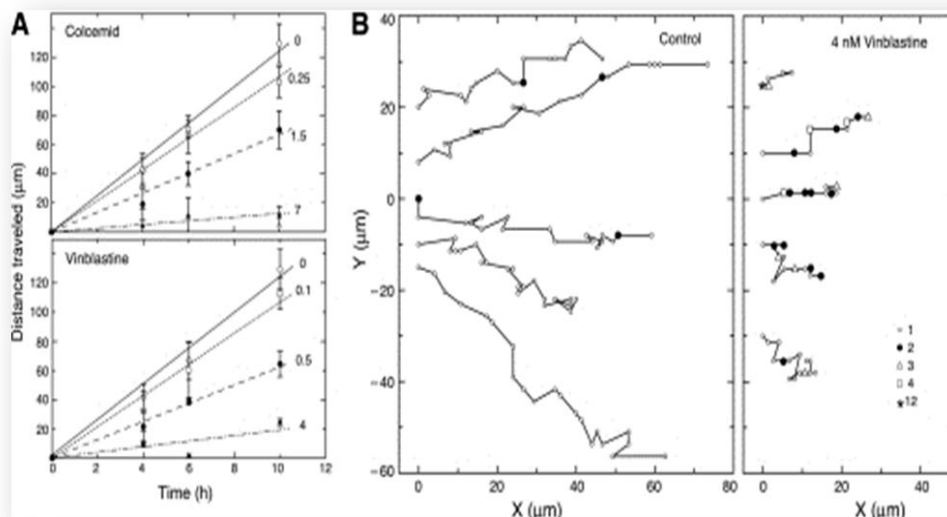
Figure 3: Effect of Drugs on Cell Migration: *A*, CHO cells were treated with colcemid or vinblastine, and the distance they moved was measured using a wound healing assay. Each line is labeled with the nM drug concentration used in the experiment. Each data point and *error bar* represents the mean ± S.D. of at least four independent experiments. *B*, control CHO cells or cells treated with 4 nM vinblastine were tracked while moving into a wound (situated toward the *right*). Each *line* represents a single cell. The *x* and *y* coordinates of the cell nucleus were measured every 15 min relative to a fixed position on the dish and plotted onto the graphs. Each *small open circle* represents a single 15-min time point. When movement did not occur after 15 min, the time points were assigned symbols according to the legend to indicate the number of 15-min intervals that passed before cell migration resumed. Thus, *filled circles* represent 2 intervals or 30 min, *open triangles* represent 3 intervals or 45 min, etc. Note that untreated cells exhibited few instances where they did not move in a 15-min time span, but vinblastine-treated cells had many such instances.

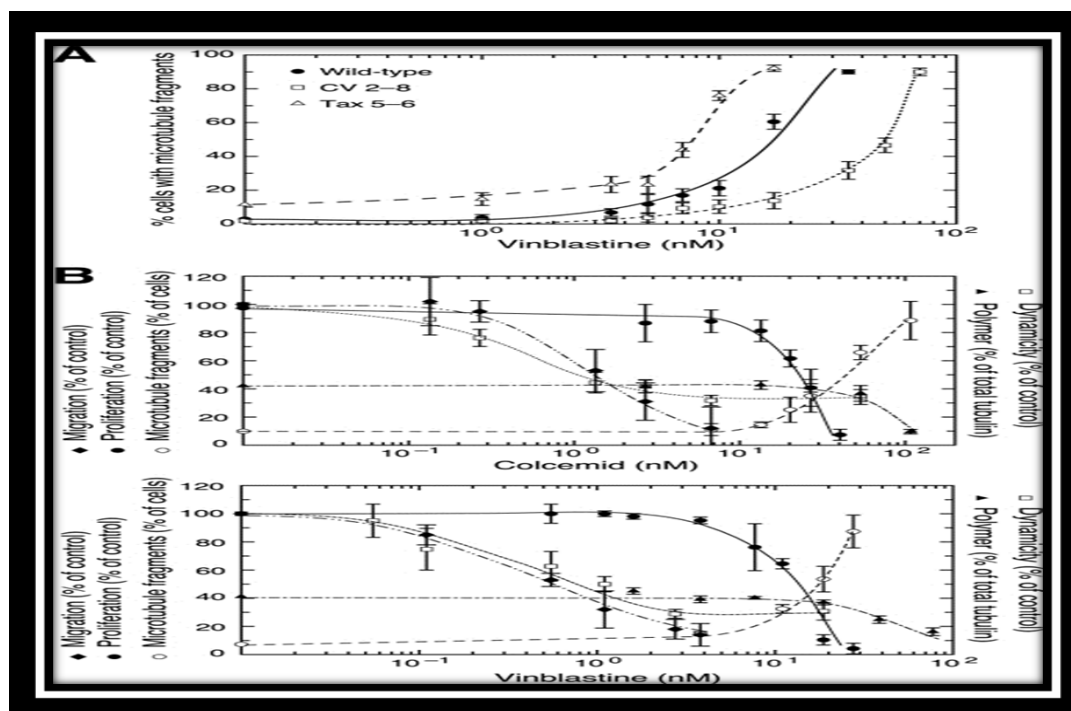**Figure 4: The appearance of microtubule fragments correlates with inhibition of cell division in wild-type and mutant CHO cells:** *A*, wild-type cells, CV 2-8, a colcemid-resistant mutant that is also 2-fold resistant to vinblastine, and Tax 5-6, a paclitaxel-resistant mutant that is 2-fold more sensitive to vinblastine, were incubated in varying concentrations of vinblastine for 2 days and stained for tubulin immunofluorescence.

The percentage of cells with >10 microtubule fragments was plotted against drug concentration for each cell line.

B, cell proliferation

Step 1: It has measured using a clonogenic assay and expressed relative to untreated cells set at 100%. The percent of cells with >10 microtubule fragments is recorded.

Step 2: In next step, the record of percent cells has been counted after treating with Colcemid or Vinblastine at the indicated concentrations for 2 days .The rate of cell migration relative to untreated control cells.

Step 3: After that, the rate of cell migration was measured using a wound healing assay that began 30 min after adding the drug.

Step 4: Microtubule dynamicity was calculated relative to untreated cells using the values found in supplemental Tables T1 and T2. The percent of total cellular tubulin found in microtubules. [**Table1** & **Table2** are shown below which are used in this process]

Step 5: At the last step, Microtubule dynamicity was measured by lysing cells in a microtubule stabilizing buffer, centrifuging to separate polymerized from non-polymerized tubulin, and quantifying the tubulin in each fraction.

Table T1: (Effects of Vinblastine on CHO microtubule dynamics).

Factors	0	0.05	0.1	0.5	1	2.5	15nM
Growth							
Rate (μm/min)	16.2 ± 0.8	16.0 ± 1.2	14.9 ± 1.8	$12.6 \pm 0.8*$	$11.8 \pm 0.6*$	$11.6 \pm 0.7*$	$10.2 \pm 0.7*$
Distance (μm)	3.2 ± 0.4	$2.0 \pm 0.2*$	2.0 ± 0.3	$1.6 \pm 0.3*$	$1.4 \pm 0.1*$	$1.2 \pm 0.2*$	$1.1 \pm 0.2*$
Duration (sec)	12.2 ± 1.2	$7.2 \pm 0.3*$	$7.8 \pm 0.9*$	$7.4 \pm 0.9*$	$7.0 \pm 0.5*$	$6.1 \pm 0.6*$	$6.3 \pm 0.4*$
SHORTENING							
Rate (μm/min)	28.2 ± 2.3	$20.4 \pm 1.3*$	$17.3 \pm 1.5*$	$17.3 \pm 1.2*$	$14.5 \pm 1.0*$	$13.3 \pm 1.2*$	$10.8 \pm 0.8*$
Distance (μm)	5.2 ± 0.6	$3.2 \pm 0.4*$	$2.5 \pm 0.4*$	$2.4 \pm 0.6*$	$2.0 \pm 0.3*$	$1.6 \pm 0.2*$	$1.3 \pm 0.1*$
Duration (sec)	11.2 ± 1.1	8.9 ± 0.8	8.0 ± 0.7	$7.3 \pm 0.7*$	$7.4 \pm 0.7*$	$7.5 \pm 0.6*$	$6.7 \pm 0.5*$
% of time in							
Growth	31.1 ± 2.2	23.7 ± 2.1	$15.6 \pm 2.6*$	$20.3 \pm 2.1*$	$17.0 \pm 1.9*$	$10.4 \pm 1.4*$	$11.4 \pm 1.9*$
Shortening	21.1 ± 1.9	20.6 ± 2.0	23.1 ± 3.3	16.5 ± 2.0	16.0 ± 2.1	$11.8 \pm 1.9*$	$13.1 \pm 1.7*$
Pause	47.8 ± 3.1	55.7 ± 3.5	$61.4 \pm 5.1*$	$63.2 \pm 3.2*$	$67.0 \pm 3.2*$	$77.8 \pm 2.5*$	$75.6 \pm 3.3*$
Frequency (min^{-1}) Catastrophe [1]	1.5 ± 0.1	1.9 ± 0.2	$2.3 \pm 0.3*$	1.8 ± 0.2	1.6 ± 0.2	1.2 ± 0.2	1.4 ± 0.2
Rescue [2]	6.3 ± 0.5	7.0 ± 0.5	7.2 ± 0.8	$9.2 \pm 0.6*$	$8.3 \pm 0.8*$	$8.5 \pm 0.7*$	$9.1 \pm 0.7*$
Dynamicity[3] (μm/min)	9.0 ± 0.9	8.6 ± 1.1	6.8 ± 1.3	$5.7 \pm 0.9*$	$4.5 \pm 0.5*$	$2.6 \pm 0.3*$	$2.8 \pm 0.5*$
Number microtubules	30	15	10	15	15	15	15

Values shown represent the mean ± s.e.m.

[1] Catastrophe: the transition from growth or pause to shortening.

[2] Rescue: the transition from shortening to growth or pause.

[3] Dynamicity: the total change of length per unit time of individual microtubules during their life histories.

$*$ $p < 0.05$ compared to 0 concentration.

Table T2: (Effects of Colcemid on CHO microtubule dynamics).

Factors	0	0.05	0.1	0.5	1	2.5	15nM
Growth							
Rate (μm/min)	16.2 ± 0.8	15.0 ± 1.2	14.1 ± 1.0	$13.0 \pm 1.1*$	$11.0 \pm 0.7*$	$10.1 \pm 0.5*$	$12.0 \pm 0.8*$
Distance (μm)	3.2 ± 0.4	$2.0 \pm 0.2*$	$1.6 \pm 0.1*$	$1.5 \pm 0.2*$	$1.2 \pm 0.1*$	$1.1 \pm 0.1*$	$1.3 \pm 0.1*$
Duration (sec)	12.2 ± 1.2	$7.8 \pm 0.5*$	$7.3 \pm 0.6*$	$6.6 \pm 0.5*$	$6.5 \pm 0.4*$	$6.7 \pm 0.4*$	$6.6 \pm 0.5*$
SHORTENING Rate (μm/min)	28.2 ± 2.3	21.9 ± 1.7	$16.6 \pm 1.5*$	$15.4 \pm 1.9*$	$15.7 \pm 1.0*$	$14.2 \pm 1.5*$	$12.5 \pm 0.8*$
Distance (μm)	5.2 ± 0.6	$3.2 \pm 0.4*$	$2.3 \pm 0.3*$	$1.9 \pm 0.3*$	$1.9 \pm 0.2*$	$1.5 \pm 0.1*$	$1.6 \pm 0.2*$
Duration (sec)	11.2 ± 1.1	8.3 ± 0.6	8.4 ± 0.6	$7.3 \pm 0.5*$	$7.1 \pm 0.5*$	$6.6 \pm 0.4*$	7.5 ± 0.6
% of time in Growth	31.1 ± 2.2	$22.13 \pm 2.2*$	$17.3 \pm 2.9*$	$10.3 \pm 1.4*$	$12.0 \pm 1.4*$	$13.3 \pm 2.0*$	$10.3 \pm 1.1*$
Shortening	21.1 ± 1.9	20.3 ± 2.0	23.1 ± 2.8	16.6 ± 1.7	$15.7 \pm 0.9*$	$12.7 \pm 1.3*$	14.8 ± 2.2
Pause	47.8 ± 3.1	57.4 ± 3.6	$59.6 \pm 5.1*$	$73.1 \pm 2.7*$	$72.3 \pm 1.6*$	$72.5 \pm 2.9*$	$75.4 \pm 2.4*$
Frequency (min^{-1}) Catastrophe [1]	1.5 ± 0.1	1.9 ± 0.2	$2.3 \pm 0.3*$	$1.7 \pm 0.2*$	1.7 ± 0.2	1.4 ± 0.2	1.5 ± 0.2
Rescue[2]	6.3 ± 0.5	7.2 ± 0.7	7.0 ± 0.7	$8.4 \pm 0.7*$	8.2 ± 0.7	$9.5 \pm 0.5*$	$8.6 \pm 0.5*$
Dynamicity[3] (μm/min)	9.0 ± 0.9	8.1 ± 1.0	6.9 ± 0.6	$4.0 \pm 0.7*$	$3.8 \pm 0.4*$	$2.9 \pm 0.3*$	$3.1 \pm 0.5*$
Number microtubules	30	16	12	15	10	10	11

Values shown represent the mean ± s.e.m.

[1] Catastrophe: the transition from growth or pause to shortening.

[2] Rescue: the transition from shortening to growth or pause.

[3] Dynamicity: the total change of length per unit time of individual microtubules during their life histories.

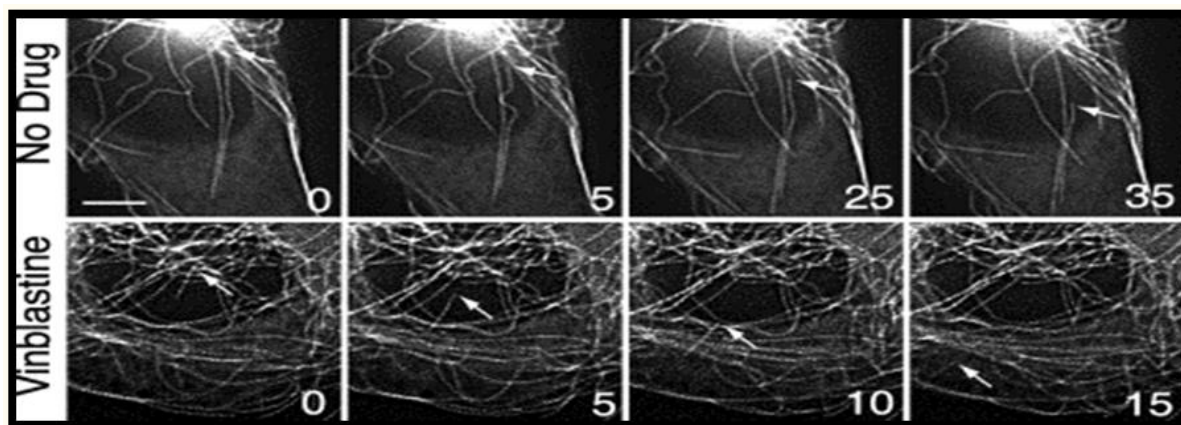$*$ $p < 0.05$ compared to 0 concentration

Figure 5: Microtubule detachment during Interphase. CHO cells transfected with EGFP-MAP4 were left untreated (upper panels) or were treated 30 min with 15 nm vinblastine, the IC50 concentration for inhibition of cell division (lower panels). Fluorescence microscopic photographs, taken 5 seconds apart at 37 °C, were deconvolved to improve contrast. Arrows point to microtubule minus-ends before and after detachment. The numbers represent the time (in seconds) the images were taken relative to an arbitrary zero time point. Bar = 5 μm.
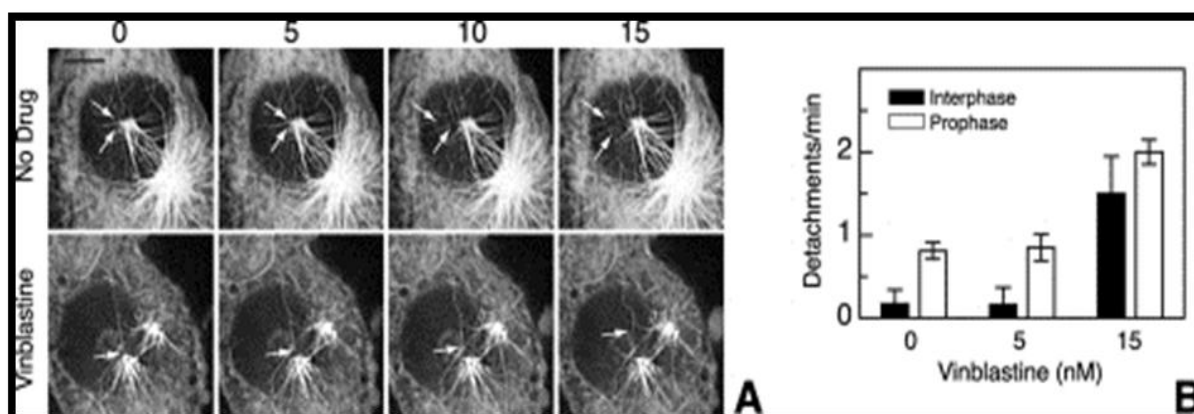

Figure 6: Microtubule detachment during mitosis. A, EGFP-MAP4-transfected CHO cells were left untreated (upper panels) or were treated 30 min with 15 nm vinblastine (lower panels) and were then viewed by live cell fluorescence microscopy. Prophase cells were located and captured every 5 seconds. The images were deconvolved to improve contrast. Arrows point to the minus-ends of microtubules that detached from the spindle poles. Bar = 5 μm. B, the number of detachments seen in control- and drug-treated prophase and interphase cells were counted from photographed images and divided by the total time of observation. The mean ± S.D. was calculated from 11–20 cells during a total observation time of 50–80 min.

Values shown represent the mean ± S.E.

	Interphase	Prophase		
	0	0	5	35 nM
Growth				
Rate (μm/min)	16.2 ± 0.8	17.1 ± 1.6	9.9 ± 0.7 [a]	12.3 ± 1.0 [a]
Distance (μm)	3.2 ± 0.4	2.5 ± 0.3	0.9 ± 0.1 [a]	1.3 ± 0.1 [a]
Duration (sec)	12.2 ± 1.2	9.0 ± 0.6	5.4 ± 0.3 [a]	6.4 ± 0.3 [a]
Shortening				
Rate (μm/min)	28.2 ± 2.3	24.6 ± 2.0	13.5 ± 1.5 [a]	13.9 ± 0.9 [a]
Distance (μm)	5.2 ± 0.6	3.3 ± 0.4	1.4 ± 0.1 [a]	1.6 ± 0.1 [a]
Duration (sec)	11.2 ± 1.1	8.7 ± 0.9	6.3 ± 0.3 [a]	6.7 ± 0.3 [a]
% Time				
Growth	31.1 ± 2.2	36.0 ± 2.4	12.2 ± 1.8 [a]	15.9 ± 2.1 [a]
Shortening	21.1 ± 1.9	33.0 ± 2.8	14.0 ± 0.8 [a]	16.3 ± 1.7 [a]
Pause	47.8 ± 3.1	31.0 ± 3.9	73.8 ± 3.9 [a]	67.7 ± 3.3 [a]
Frequency (min^{-1})				
Catastrophe [b]	1.5 ± 0.1	3.4 ± 0.3	1.6 ± 0.1 [a]	1.8 ± 0.2 [a]
Rescue [c]	6.3 ± 0.5	6.0 ± 0.5	9.3 ± 0.9 [a]	9.4 ± 0.5 [a]
Dynamicity [d] (μm/min)	9.0 ± 0.9	13.8 ± 1.4	3.1 ± 0.4 [a]	4.2 ± 0.6 [a]
Number of microtubules	30	12	8	15

Open in a separate window

[a] $p < 0.05$ compared to 0 concentration in prophase cells.

[b] The transition from growth or pause to shortening.

[c] The transition from shortening to growth or pause.

[d] The total change of length per unit time of individual microtubules during their life histories.

Figure 7: Effect of Vinblastine on microtubule dynamics in prophase CHO cells: deconvolved to improve contrast. *Arrows* point to microtubule minus-ends before and after detachment. The numbers represent the time (in seconds) the images were taken relative to an arbitrary zero time point. *Bar* = 5 μm.

RESULTS AND SOLUTIONS

- **Drugs that are to be used and will be incorporated**

1) VINBLASTINE/VINCRISTIN/VINORLBINE

Vinblastine (VBL), is chemotherapy medication, typically used with other medications, to treat various types of cancer. This includes Hodgkin's lymphoma, non-small cell lung cancer, bladder cancer, brain cancer, melanoma, and testicular cancer, It is given by injection into a vein.

- Vinblastine is a *vinca* alkaloid and a chemical analogue of Vincristine It binds tubulin, thereby inhibiting the assembly of microtubules. Vinblastine treatment causes M phase specific cell cycle arrest by disrupting microtubule assembly and proper formation of the mitotic spindle and the kinetochore, each of which are necessary for the separation of chromosomes during anaphase of mitosis. Toxicities include bone marrow suppression (which is dose-limiting), gastrointestinal toxicity, potent vesicant

(blister-forming) activity, and extravasation injury (forms deep ulcers). Vinblastine paracrystals may be composed of tightly-packed unpolymerized tubulin or microtubules.
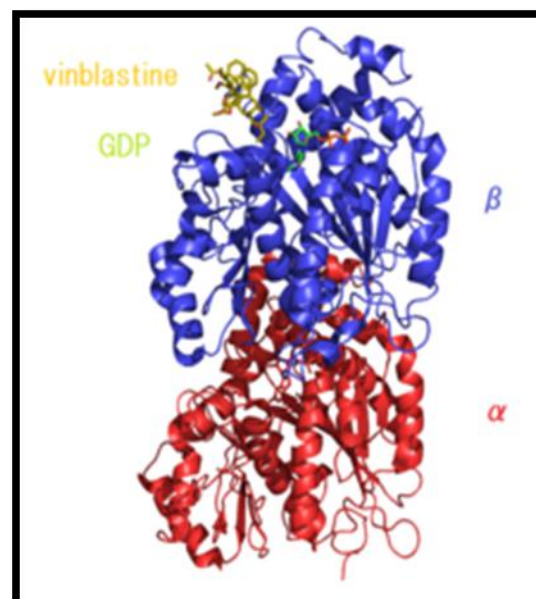

Figure 8: The complex of Tubulin and Vinblastine. (Vinblastine is shown in yellow in the figure).

2) CIS PLATIN

Cisplatin, cisplatinum, or *cis*-diamminedichloroplatinum (II), is a well-known chemotherapeutic drug. It has been used for treatment of numerous human cancers including bladder, head and neck, lung, ovarian, and testicular cancers. It is effective against various types of cancers, including carcinomas, germ cell tumors, lymphomas, and sarcomas. Its mode of action has been linked to its ability to crosslink with the purine bases on the DNA; interfering with DNA repair mechanisms, causing DNA damage, and subsequently inducing apoptosis in cancer cells.

- Carboplatin or Cis diammine (1,1-cyclobutanecarbo-xylato) platinum (II) is a chemotherapeutic drug used for cancers of ovaries, lung, head and neck. In terms of its structure, carboplatin differs from cisplatin by having a bidentate dicarboxylate (CBDCA) ligand in place of the two chloride ligands, which are the leaving groups in cisplatin. It exhibits lower reactivity and slower DNA binding kinetics, although it forms the same reaction products in vitro at equivalent doses with cisplatin. The process shall be restricted till the cell cycle arrest stage.
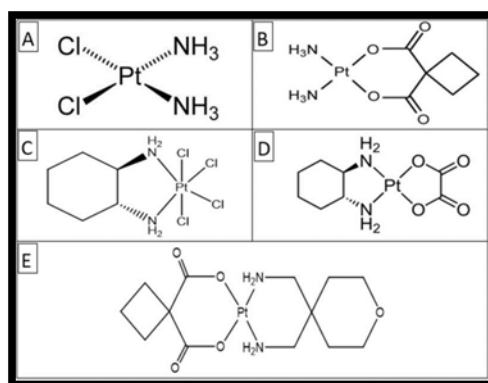- CISPLATIN is used in various cancer treatments and more effective when added up with the VINBLASTIN.

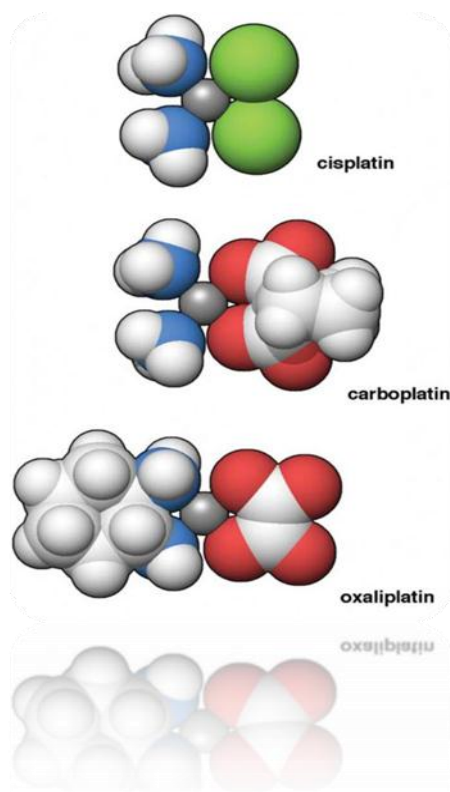**Figure 9: Chemical Structure of CISPLATIN.**

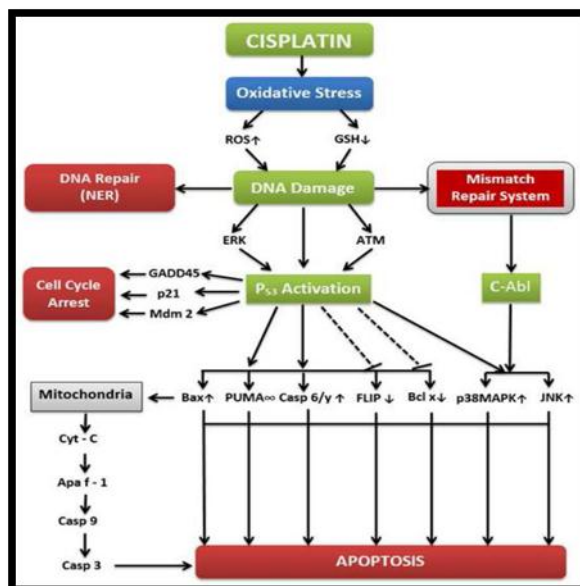**Figure 10: CISPLATIN molecular structure.**

Figure 11: Mechanism of the CISPLATIN.

Dosage, Form, Side-Effects:
- Both CISPLATIN and VINBLASTIN are given INTRAVENOUSLY.
- ➤ DOSAGE THAT ARE GENERALLY PRESCRIBED:

i) **VINBLASTIN:**

a) **General Dosing Ranges:**
- 3.7-18 mg/m²/day IV q(7-10) days
- 1st dose 3.7 mg/m²/day IV
- Increased by 1.85 mg/m² week until WBC equal 3000/mm³
- Dose range: 5.5-7.4 mg/m²
- Not to exceed 18.5 mg/m²

b) **Hodgkin's Disease:**
6 mg/m² q2weeks; part of combination treatment

c) **Testicular Cancer:**
6 mg/m²/day x 2 days q(3-4) weeks; part of combination treatment

d) **Bladder Cancer:**
3 mg/m² q7d x 3 out of 4week; part of combination treatment

e) **Melanoma:**
2 mg/m² days 1-4 & 22-25 of 6week cycle

f) **Non-small Lung Cancer:**
4 mg/m²/day on days 1,8,15,22, 29, then q 2week; part of combination treatment

g) **Ovarian Cancer:**
0.11 mg/kg/day x 2 days q 3week; part of combination treatment

h) **Prostate Cancer:**
4mg/m²/week x 6 weeks of 8 week cycle

ii) **CISPLATIN:**

a) **Injectable Solution:**
1mg/ml

b) **Metastatic Testicular Tumors:**
20 mg/m²/day IV for 5 days repeated every 3 weeks (in combination with bleomycin and etoposide)

c) **Advanced Bladder Cancer:**
- 50-70 mg/m² IV cycle q3-4Weeks, depending on prior radiation therapy or chemotherapy
- Heavily pretreated patients: 50 mg/m²/cycle initially; repeat q4Weeks

d) **Metastatic Ovarian Carcinoma:**
75-100 mg/m² IV per cycle q4Weeks with cyclophosphamide (600 mg/m² IV q4Weeks); administer sequentially Off-label: 90-270 mg/m² intraperitoneal; retain for 4 hr before draining; repeat q3Weeks (may co-administer systemic Na-thiosulfate).

e) **Cancers (Off-label):**
- Cancer of cervix, endometrium, prostate, esophagus, kidney; non-small cell lung cancer; head & neck squamous cell cancer; osteogenic sarcomas; bone marrow transplants 75-100 mg/m² IV q4Weeks when used with cyclophosphamide
- 100 mg/m² IV q4Weeks as single agent.

- **Side Effects**
1) **VINBLASTIN**
- Low blood counts.
- Injection site reactions
- Fatigue, and weakness

2) **CISPLATIN**
- nausea and vomiting (may be severe),
- diarrhea,
- temporary hair loss,
- loss in ability to taste food,
- hiccups,
- dry mouth,
- dark urine,
- decreased sweating,
- dry skin, and
- other signs of dehydration.

- **To Counteract The Side Effects, Preferred Drugs Are To be Prescribed along with the Main two Drugs (Vinblastin And Cisplatin).**
- **DRUG MODIFICATION**
- Our prime aim is to make a drug using both **VINBLASTIN** and **CISPLATIN** and to **integrate with the NANOBOTS** which will kill the cancer cells from inside by a process similar to induced apoptosis.
- The side effects should be thoroughly examined and the preferred drugs prescribed.

- **DOSAGE CALCULATION**
- ➢ Desired Over Have or Formula Method

Desired over Have or Formula Method is a formula or equation to solve for an unknown quantity (x) much like ratio proportion. Drug calculations require the use of conversion factors, such as when converting from pounds to kilograms or liters to milliliters. Simplistic in design, this method allows us to work with various units of measurement, converting factors to find our answer. Useful in checking the accuracy of the other methods of calculation as above mentioned, thus acting as a double or triple check.

- A basic formula, solving for x, guides us in the setting up of an equation:
- D/H x Q = x, or Desired dose (amount) = ordered Dose amount/amount on Hand x Quantity.
- INTRAVENOUS CALCULATION

[Amount of fluid to be infused] x [drop factor] ÷ minutes to infuse = gtts/min

Identification of the Mutated Cells & Genomes and Marking with Suitable Markers

Here is the set of process for identification of Mutated Cells and their pathways which results the Cancer and marking them for Drug application with the Nanobots technology:

1) Non coding somatic genomes mutation Analysis

Here is the graph showing frequency of Pan Cancer Analysis of Whole Genomics (PCAWG) datasets, where more than 2600 cancer genomes mutation pattern has been achieved. In this graphs it shows different mutational process happens and also the nature and consequences of somatic and germline variations in both coding and non-coding regions, with specific emphasis on cis-regulatory sites, non- coding RNAs and large – scale structural alternations. For point mutations, we developed a statistically rigorous strategy for combining significance levels from multiple methods of driver discovery that overcomes the limitations of individual methods. For structural variants, we present two methods of driver discovery, and identify regions that are significantly affected by recurrent breakpoints and recurrent somatic juxtapositions. Our analyses confirm previously reported drivers 6, 7 raise doubts about others and identify novel candidates, including point mutations in the 5' region of TP53, in the 3' un-translated regions of NFKBIZ and TOB1, focal deletions in BRD4 and rearrangements in the loci of AKR1C genes. We show that although point mutations and structural variants that drive cancer are less frequent in non-coding genes and regulatory sequences than in protein-coding genes, additional examples of these drivers will be found as more cancer genomes become available. This 2nd graph (below) shows the translation process on various driver site points with their mutations number affecting to produce the protein with number of hits.
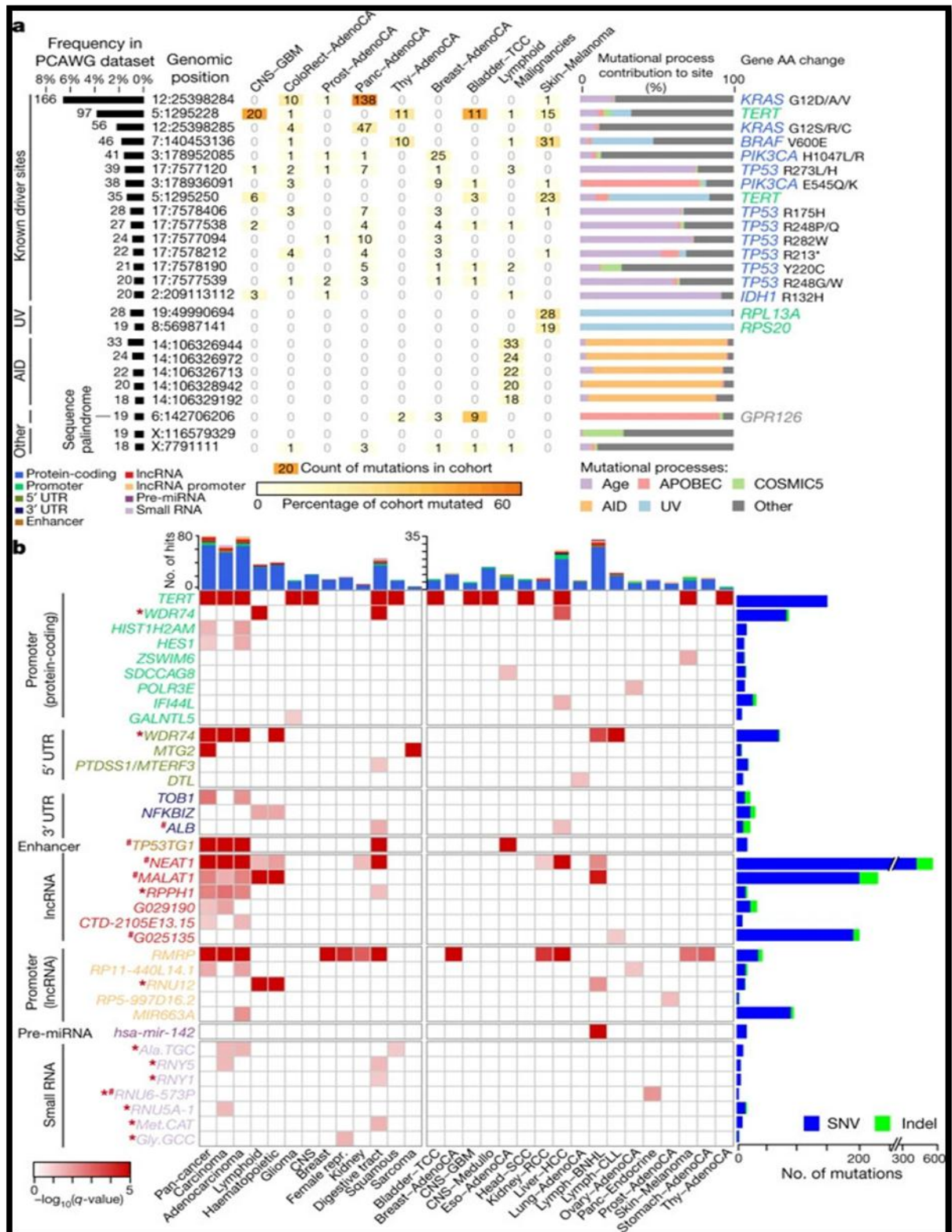
Figure 12: Noncoding Somatic Gene Mutation.

2) **Marking the mutated genes and their pathway and protein for Analysis**
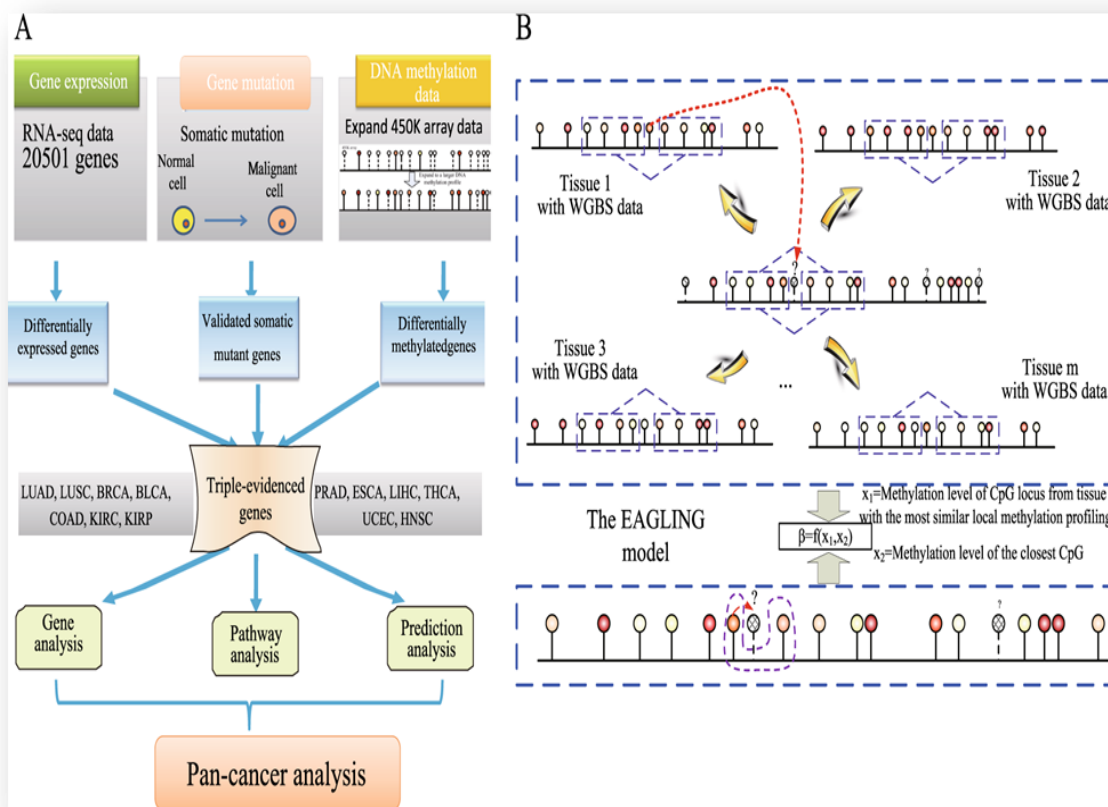
Figure 13: Marking and pathway of Mutated Genes.

This figure (figure 13) shows how we can analysis the triple-evidenced to get about gene mutation. This process not only helps to get information about the gene and their pathway also generated protein analysis to get the data to select the gene marker for future cancer enhancement and to destroy it critically with the Nanobots. We can also use the Data from one such source, the Genetic Alterations in Cancer (GAC) database (http://dirapps.niehs.nih.gov/gac/). The GAC database was developed by National Institute of Environmental Health Sciences as a web-based system for collecting and summarizing data reported in the published literature for genetic alterations in various types of human cancers and laboratory rodent tumors. It provides a unique tool for assessing groups of related genes for mutations, allelic loss and homozygous deletions based on species and tumor site. Tumor morphologies from different topographical sites (regions of the body) and exposures to environmental agents can also be distinguished. Collating these types of data allows a broader view of tumor development and facilitates comparative analysis of multiple genes in genetic pathways to cancer rather than focusing on single genes. We can also easily illustrate, how changes in specific genes, and different patterns of gene alterations in various topographical sites, may serve as markers of exposure.

TruSight Cancer 94-Gene pre-disposition Panel for detecting Germline mutations									
AIP	BUB1B	DDB2	EXT2	FANCL	MEN1	PALB2	RB1	SLX4	WRN
ALK	CDC73	DICER1	EZH2	FANCM	MET	PHOX2B	RECQL4	SMAD4	WT1
APC	CDH1	DIS3L2	FANCA	FH	MLH1	PMS1	RET	SMARCB1	XPA
ATM	CDK4	EGFR	FANCB	FLCN	MSH2	PMS2	RHBDF2	STK11	XPC
BAP1	CDKN1C	EPCAM	FANCC	GATA2	MSH6	PRF1	RUNX1	SUFU	
BLM	CDKN2A	ERCC2	FANCD2	GPC3	MUTYH	PRKAR1A	SBDS	TMEM127	
BMPR1A	CEBPA	ERCC3	FANCE	HNF1A	NBN	PTCH1	SDHAF2	TP53	
BRCA1	CEP57	ERCC4	FANCF	HRAS	NF1	PTEN	SDHB	TSC1	
BRCA2	CHEK2	ERCC5	FANCG	KIT	NF2	RAD51C	SDHC	TSC2	
BRIP1	CYLD	EXT1	FANCI	MAX	NSD1	RAD51D	SDHD	VHL	

Figure 14: Detection of Germline Mutations.

3) Germline mutations cancer causing genes description

This image (figure 14) shows how we learn more about the role genetic variants play in cancer predisposition, we will need to be able to evaluate the genes in which these variants lie comprehensively. This process is now simpler and faster with the TruSight Cancer Sequencing Panel. Developed in collaboration with experts in cancer genomics, the predesigned, ready-to-use oligos specifically target genes associated with cancer. The sequencing panel is compatible with TruSight Rapid Capture kits, providing a single and integrated library preparation. Delivering excellent data quality from low sample input (50 ng), TruSight Cancer and TruSight Rapid Capture enable researchers to analyze precious samples, while retaining sufficient material for future analyses.

4) Finding Cancer-critical genes for readily use markers

Cancer is a genetic disease: it results mainly from mutations in somatic cells. To understand it at a molecular level, we need to identify the relevant mutations and to discover how they give rise to cancerous cell behavior. Finding the mutations is easy in one respect: the mutant cells are favored by natural selection and call attention to themselves by giving rise to tumors. The hard task then begins: how are the genes with the carcinogenic mutations to be identified among all the other genes in the cancerous cells? A similar needle-in-haystack problem arises in any search for a gene underlying a given mutant phenotype, but for cancer the task is particularly complex. A typical cancer depends on a whole set of mutations—usually a somewhat different set in each individual patient—and introduction of any single one of these into a normal cell is usually not enough to make it cancerous. This genetic cooperation makes it hard to test the significance of mutations on which suspicion falls. To make matters worse, most cancer cells will contain mutations that are accidental by-products of genetic instability, and it can be difficult to distinguish these from the mutations that have a causative role in the disease.
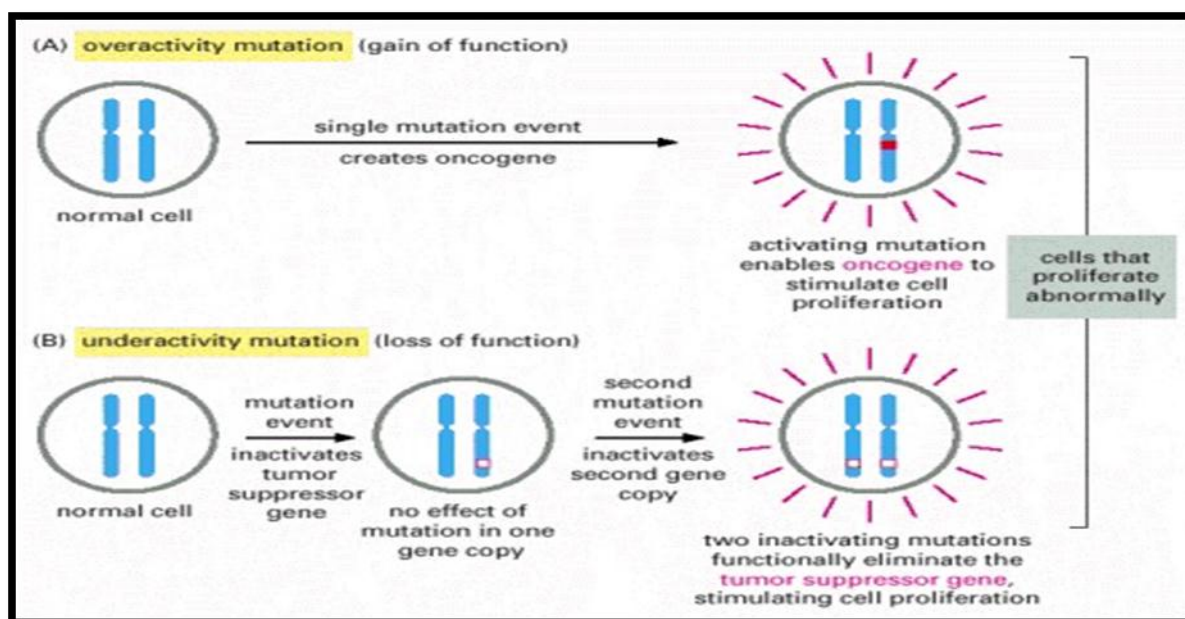

Figure 15:

This figure shows how "Cancer-critical genes fall into two readily distinguishable categories, dominant and recessive"

Oncogenes act in a dominant manner: a gain-of-function mutation in a single copy of the cancer-critical gene can drive a cell toward cancer. Tumor suppressor genes, on the other hand, generally act in a recessive manner: the function of both alleles of the cancer-critical gene must be lost to drive a cell toward cancer. In this diagram, activating mutations are represented by solid red boxes, inactivating mutations by hollow red boxes.

5) Screening for multiple different cancers within the general population

Most cancers are detected when they cause symptoms that lead to medical evaluation. Unfortunately, in too many cases this results in diagnosis of cancers that are locally invasive or already metastatic and hence no longer curable with surgical resection or radiation treatment. Medical therapies, which might be curative in the setting of minimal tumor burden, typically provide more limited benefit in more advanced cancers, given the emergence of drug resistance. CancerSEEK involves "the use of a unique, non-invasive, multi-analyte test that simultaneously evaluates the presence of mutations and eight cancer-associated protein biomarkers in blood".

Multiplex PCR analysis of circulating cell-free tumour DNA (ctDNA) enables the detection of mutations at 2,001 genomic positions across 16 genes, whereas levels of the protein biomarkers are assessed using immunoassays. As each marker does not have sufficient sensitivity to be used alone to detect cancer, the multi-analyte approach markedly increases the test sensitivity. Application of a supervised machine-learning algorithm to the multi-analyte data enabled the organ of origin to be correctly identified in a median of 63% of the patients with a positive CancerSEEK test, and in a median of 83%, the cancer site was within the top two predicted locations. The accuracy of the predictions varied by tumour type, and was high for colorectal, ovarian, and pancreatic cancers (~80%), but markedly lower for upper Gastro-intestinal, liver, and lung cancers (~40%).
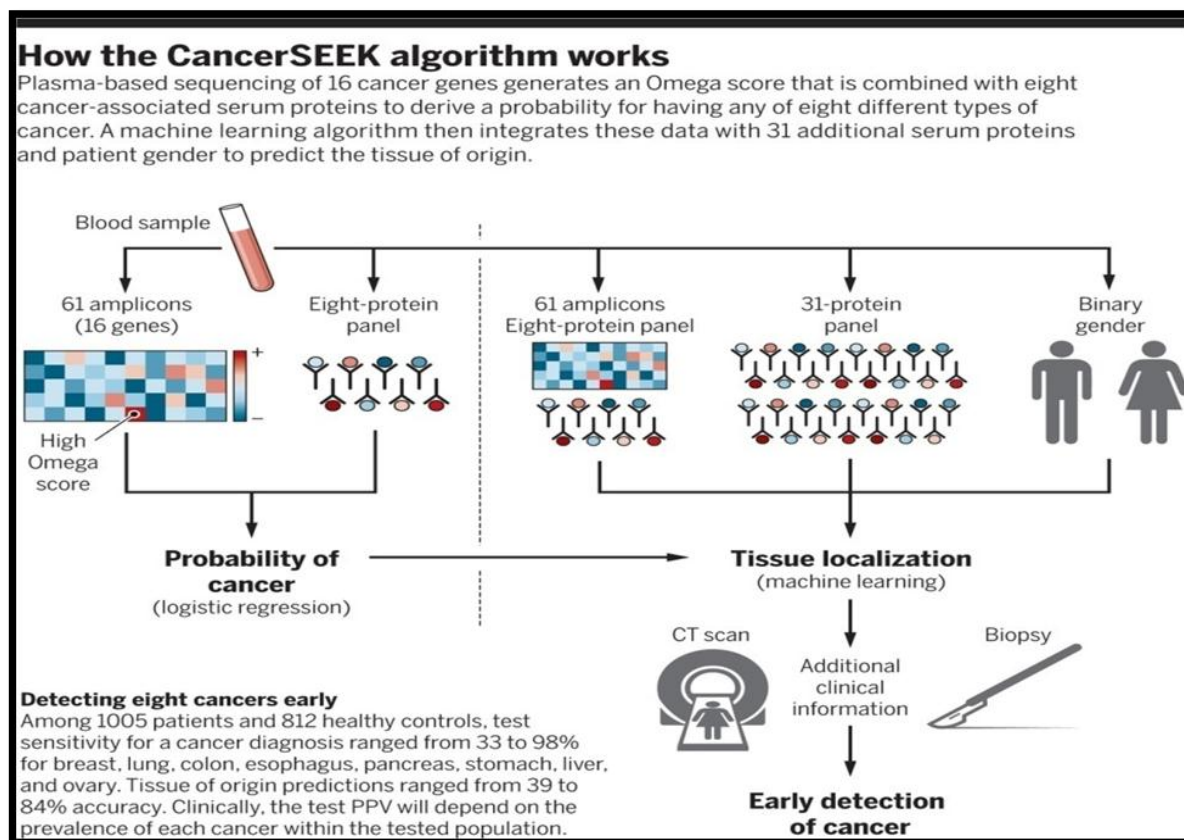

Figure 16: Algorithm for Cancer detection.

6) Ranking of cancer point mutations in MutaGene

MutaGene webserver provides a collection of cancer-specific context-dependent mutational profiles. It allows to calculate the nucleotide and codon mutability and B-Score for missense, nonsense and silent mutations for any given protein coding DNA sequence and background mutagenesis model using the "Analyze gene" option. Mutations with the B-Score below the first threshold are predicted to be "cancer drivers", whereas mutations with scores in between two thresholds are predicted to be "potential drivers". All mutations with scores above the second threshold are predicted as "passengers". Importantly, calculations are not limited to pan-cancer and can be performed using a mutational profile for any particular cancer type, the latter would result in a cancer-specific ranking of mutations and could be useful for identification of driver mutations in a particular type of cancer.
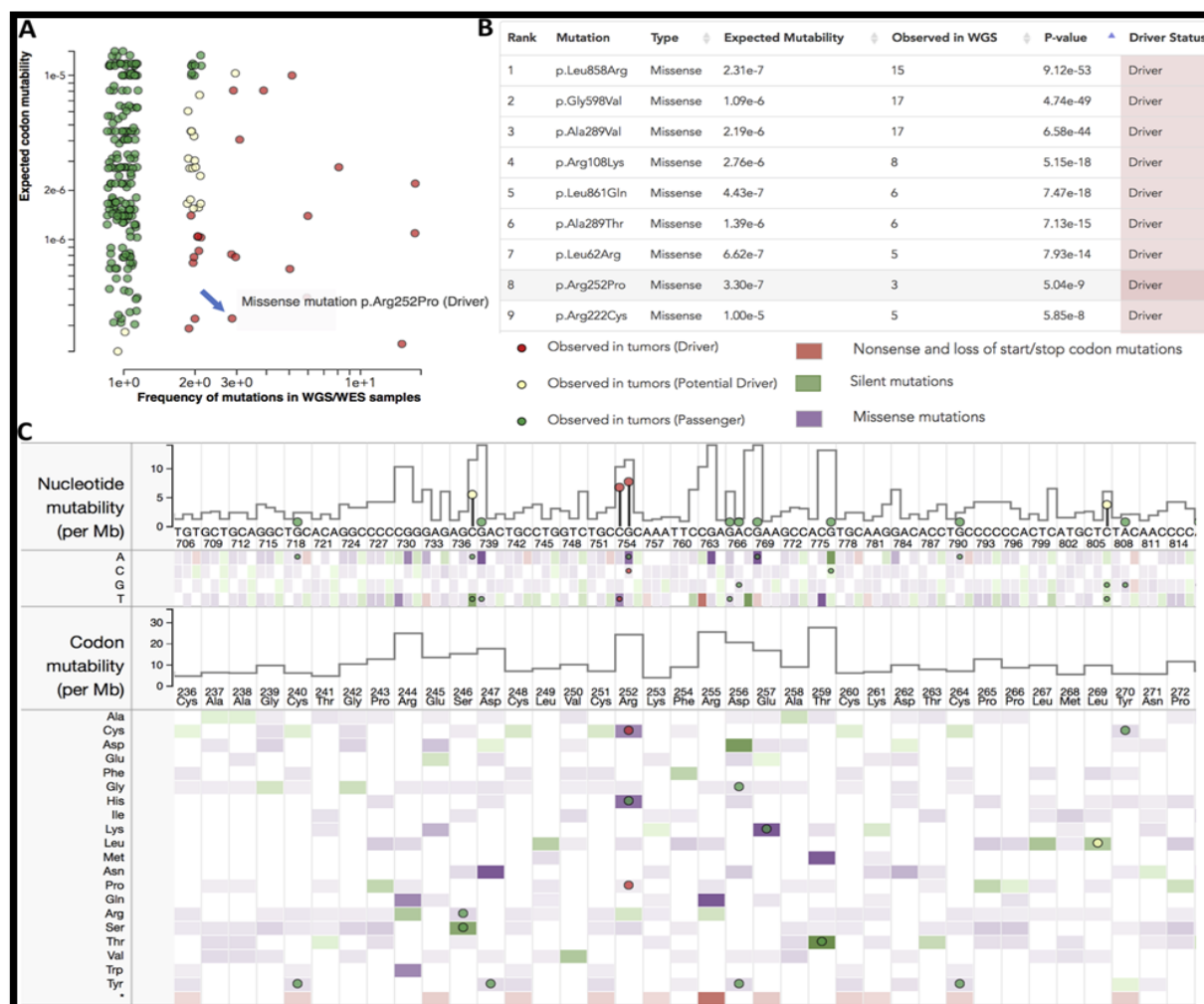
Figure 17: Ranking of Mutation by MutaGene Python.

MutaGene Python package allows to rank the mutations in a given sample or cohort in a batch mode using pre-calculated or user-provided mutational profiles or signatures and is available at https://www.ncbi.nlm.nih.gov/research/mutagene/gene.
There are two different ways to load files in Mutagen, but both provide similar interfaces like the first is the Metadata API, which deals only in metadata tags and the second is the FileType API, which is a superset of the Metadata API, and contains information about the audio data itself. Both Metadata and FileType objects present a dict-like interface to edit tags. FileType objects also have an 'info' attribute that gives information about the song length, as well as per-format information. In addition, both support the load(filename), save(filename), and delete(filename) instance methods; if no filename is given to save or delete, the last loaded filename is used. So, we can easily use it to rank the mutation gene and further calculations about it to identify.

7) Protein dynamics to identify cancer mutational hotspots using 3D structures
The identification of cancer drivers is essential for realizing the goal of precision medicine in cancer. By integrating 3D protein structures and dynamics, we describe a framework to identify cancer driver genes using a sensitive search of mutational hotspot communities in 3D structures.

As expected, we observed a relatively higher number of genes with at least 1 hotspot community on the pan-cancer level compared to cancer-specific analysis. Our pan-cancer analysis identifies hotspot communities in protein structures of 434 unique genes (in the below figure). In contrast, a cancer-specific analysis revealed 56 potential driver genes with 186 significantly mutated hotspot communities in the corresponding protein structure. Some of these genes (including *TP53*, *PIK3CA*, *BRAF*, *SPOP*, *KRAS*, *HRAS*, and *PTEN*) have previously been shown to be drivers for different cancer types. However, we also identified numerous genes containing hotspot communities that might drive cancer progression. Previous studies suggest that newly identified driver genes, including *RHOC*, *NCOA1*, and *KLHL12*, are involved in various signaling pathways. Similarly, *PSPC1*, *FOXO3*, and *XRCC5* are known to be pivotal for immune response, apoptosis, and DNA repair, respectively. Furthermore, among these 434 genes, 12 had 5 or more hotspot communities, whereas 352 genes had just 1

hotspot community. These results highlight the efficacy of our approach in identifying novel and low-frequency putative driver genes with hotspot communities. Mutational cluster-based approaches assume that residues constituting such clusters are essential for protein function. Thus, a majority of cancer missense mutations occupying these hotspot communities are very likely to disrupt the protein functionality. In order to validate this assumption, we quantified the cross-species conservation measure [PhyloP score] for mutations in hotspot as well as non-hotspot communities. As expected, we observe higher average conservation scores for mutations associated with residues in hotspot communities compared to those outside of hotspots. Furthermore, the observed difference in conservation was statically significant (2-sided KS test, $P < 2e\text{-}5$). Similarly, the putative molecular functional impact [CADD score of mutations occupying hotspot communities was significantly higher compared to those mapping to non-hotspot communities (2-sided KS test, $P < 2e\text{-}5$). Large-scale exome sequencing of tumors has enabled the identification of cancer drivers using

recurrence and clustering-based approaches. These methods also employ three-dimensional protein structures to identify mutational hotspots in cancer-associated genes. In determining such mutational clusters in structures, existing approaches overlook protein dynamics, despite the essential role of dynamics in protein functionality. So, here we are presenting a framework to identify driver genes using a dynamics-based search of mutational hotspot communities. After partitioning 3D structures into distinct communities of residues using anisotropic network models, we map variants onto the partitioned structures. We then search for signals of positive selection among these residue communities to identify putative drivers. We applied our method using the TCGA pan-cancer atlas mis-sense mutation catalog. Ontological and pathway enrichment analyses implicate genes with predicted hotspots to be enriched in biological processes associated with tumor progression. The approach of the hotspot detection methods that use structural data suggests that the inclusion of dynamics significantly increases the sensitivity of driver detection.
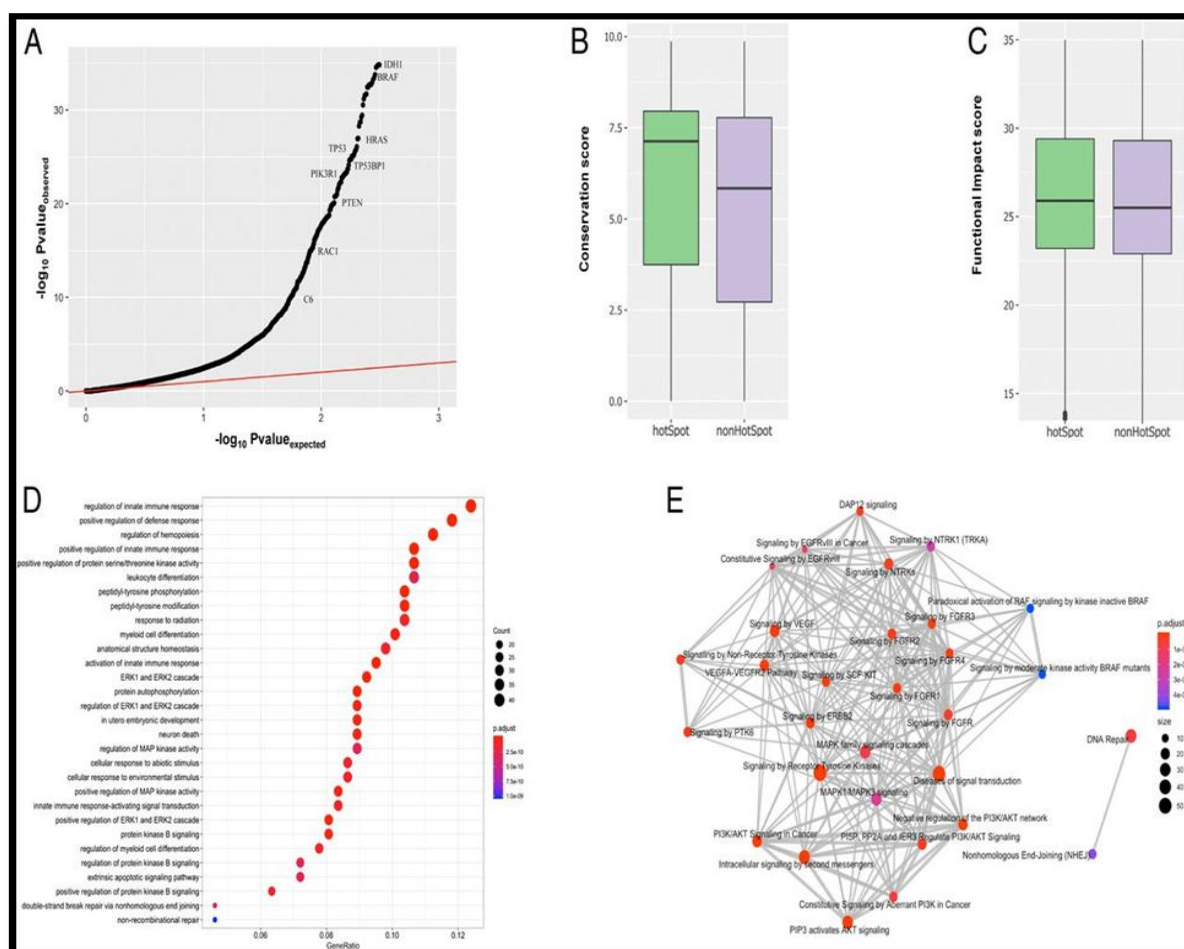

Figure 18: Mutation Hotspot 3D Analysis.

8) Mutation Data Scoring Technique for targeting Cancer Drug
MDS approach is to simulate all known protein coding genes as the putative drug targets. The model used was

built on the basis of 18,273 mutation profiles from COSMIC database for eight cancer types. We can find that the MDS algorithm-predicted hits frequently coincide with those already used as targets of the existing

cancer drugs, but several novel candidates can be considered promising for further developments. We can use the MDS for ranking of anticancer drugs and can be applied for the identification of novel molecular targets. The principle of ***Mutation Drug Scoring (MDS)*** methods proposed here deals with quantization of mutation enrichment for the molecular pathways having molecular targets of a drug under investigation. Overall, they are based on the rationale that the greater is the mutation level of the respective pathways, the higher will be the expected drug efficiency. The mutation enrichment of a molecular pathway called pathway instability (*PI*) is calculated based on the relative *mutation rates* (*MR*) of its member genes. Under *mutations*, we meant here the changes in protein coding sequence understood as such in the Catalog of Somatic Mutations in Cancer (COSMIC) v.76 database (Forbes et al., 2016). COSMIC is the world's largest database of somatic mutations relating to human cancers. We used only Genome-wide Screen Data to estimate *MR* correctly.

Mutation rate (*MR*) is calculated according to the formula:
MRn,g=N mut(n,g)N samples (g),

where $MR_{n,g}$ is *MR* of a gene *n* in a group of samples *g*; *N mut(n,g)* is the total number of mutations for gene *n* in a group of samples *g*; *N samples (g)* is the number of samples in a group *g*. The *MR* values strongly positively correlated with the lengths of gene coding DNA sequence (CDS; data not shown). In order to remove bias linked with the CDS length, we took for further consideration a normalized value termed *Normalized Mutation Rate* (*nMR*) expressed by the formula:
nMRn=1000∗MRnLength CDS (n),

where, nMR_n is the *nMR* of a gene *n*; MR_n is the *MR* of a gene *n*; *Length CDS(n)* is the length of CDS of gene *n* in nucleotides. Indeed, normalization of this metric enabled to terminate any CDS-linked bias.

To determine if gene *n* is included in pathway *p*, we introduced a Boolean flag *pathway-gene indicator* $PG_{n,p}$ expressed by the formula:
PGn,p= {1, pathway p includes gene n,0, pathway p doesn′t include gene n;

The *Pathway Instability* (*PI*) score is then calculated as follows:
PIp=∑nnMRnPGn,p,

Where, PI_p is pathway instability score for a pathway *p*; nMR_n is the *normalized* mutation rate of a gene *n*, $PG_{n, p}$ is pathway-gene indicator for gene *n* and pathway *p*. *Pathway instability score* characterizes the mutation enrichment of a pathway (Pathway instability is an effective new mutation-based type of cancer biomarkers, 2018, in preparation). To formalize if

gene *n* is molecular target of drug *d*, we introduced another Boolean flag *drug target index*, $DTI_{d, n}$:
DTId,n={1, drug d has target gene n,0, drug d doesn′t have target gene n

To complete *DTI* database for this study, we used the data about molecular specificities of 128 target drugs extracted from the databases DrugBank (Law et al., 2014) and Connectivity Map (Lamb et al., 2006).

To link *PI* scores and estimated drug efficiencies, the following basic formula was proposed for the calculation of *Mutation Drug Score* (*MDS*):
MDSd=∑nDTId,n∑pPGn,pPIp,

where *d* is drug name; *n* is gene name; *p* is pathway name; MDS_d is *MDS* for drug *d*; $DTI_{d,n}$ is drug target index for drug *d* and gene *n*; PI_p is *Pathway Instability* of pathway *p*; $PG_{n,p}$ is pathway-gene indicator for gene *n* and pathway *p*.
The above basic formula (*1*) was modified to generate several alternative methods of drug scoring.

- *-Pathway size-normalized*. Since molecular pathways include considerably different number of genes varying from dozens to hundreds, we proposed a modification of the calculation method (*1*) where normalization is performed for *MDS* on the respective number of genes for each *PI* member:
MDS_Nd=∑nDTId,n∑pPGn,pPIp/kp,

Where, k_p is number of genes in pathway *p*.
- *- Single count-normalized*. Impact of each gene participating in pathways targeted by drug *d* is counted only once:
MDS_gened=∑nnMRn GIId,n,

Where, $GII_{d, n}$ – Boolean flag *gene involvement index*,
GIId,n={1, gene n participates in at least one pathway ta rgeted by drug
d0, gene n doesn′t participate in pathways targeted by dr ug d

- *- Number of pathways-normalized*. *MDS* for drug *d* is normalized on the number of its targeted molecular pathways.
MDS_md=MDSd/md,
Where, m_d – number of pathways targeted by drug *d*.

- *- Number of pathways-normalized*. *MDS_N* is additionally normalized on the number of pathways targeted by drug *d* (m_d).
MDS_N_md=MDS_N/md
- *- Number of target genes-normalized*. MDS_b_d is additionally normalized on the number of target genes for drug *d*, (b_d).
MDS_bd=MDSd/bd
- *- Number of target genes-normalized MDS_N*. *MDS_N*, normalized on the number of target genes for drug *d*, (b_d).

MDS_N_bd=MDS_N/bd

- *- Number of target genes-normalized MDS_gene. MDS_gene, normalized on the number of target genes for drug d, (b_d).*

MDS_gene_bd=MDS_gene/bd

- *- Target genes dependent only. MDS2 is calculated considering only mutation frequencies of target genes.*

MDS2d=∑pPGn,p ∑nDTId,nnMRn

- *- Single count-normalized, target genes dependent only. MDS2_gene is calculated, considering each target gene for drug d only one time.*

MDS2_gened=∑nDTId,n NMRn GIId,n

For these algorithms of mutation-based drug scoring, we have to compare this with the published clinical trials data.

Usage of Nanobots (Biological) in Cancer Drug Deliveries

- **Preferred Medium**

1) NanoCapsules
2) Biodegradable Nanorobots

A) NanoCapsule Usage

- **Overall Structure:** Bacteriophage
- **Definition:** According to IUPAC; Hollow nanoparticles composed of a Solid Shell that surrounds a core-forming space available to entrap substances.
- **Structure:** For the cover of Capsule part, Nanocapsule Structure consists of non vesicular system that is formed in a coreshell arrangement. The shell of typical nanocapsules is made of a typical polymer i.e. coating. The polymers used are biodegradable.
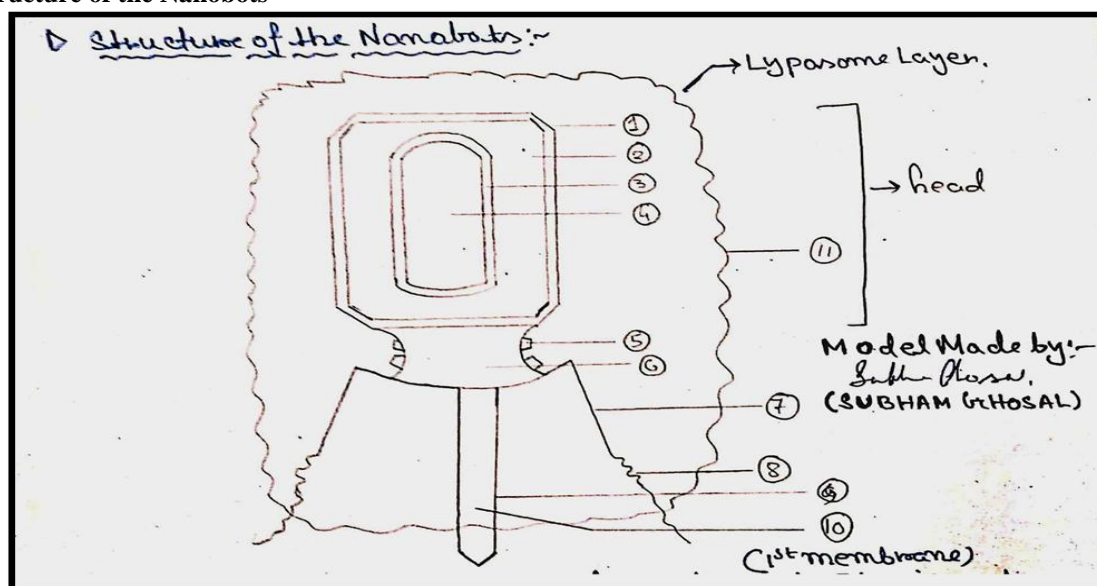
- **Structure of the Nanobots**

- **Preferred Structure Components and Polymers**

We prefer to use "Chemically Controlled Systems", it means biodegradable, and can be controlled by pH or temperature.

a) Poly ε-Caprolactone. (one of the cheapest Capsule material)
b) Poly(lactic/glycolic acid)
c) Poly(anhydries)
d) Polyorthoesters etc., these polymers gives degradation tasted on hydrolytic cleavage of ester bonds or ester derivatives.

All the above materials work on Hydrolysis.

We can also use the polymers, which give response to the external electrical stimuli.

These are:

- **Polythiophene(PT) or Sulphonated Polystyrene.**
- **Important Characteristics:** This can also be used as sensors.
- **Charge storer:** As charge storer or Electrical impulse given, we can use ATP.
- **Cell Gripper**

a) Protein filaments (similar as in phages). (preferred)
b) Modified molecules with an affinity towards the biomarker of the Cancer Cells. (Highly preferred)
c) Chitin

- **Repairing Drugs inside the Vector**

a) Vinblastin (from stopping cell division)
b) Cisplatin (for Apoptosis/ if needed)
c) Endonuclease, or Rertrictare (For DNA Splicing)
d) Taq (Thermus Aquaticus) polymer (for Fresh DNA generation)

First two are used in first stage and last two are used in second stage.

Figure 19: Hand-drawn Nanobot Structure Proposed By Subham Ghosal.

Description

1) Electric Pulse Stimulated membrane (1st membrane)

It will get dissolved when it will get a certain amount of electric pulse, stored in the electric charge storer. (6)

2) Intermembranous place

Here will be stored the Vinblastin and Cisplastin mixture. When, (1) will be ruptured, there components will be released.

3) pH Stimulated Membrane (2nd membrane)

It will get ruptured when it will be exposed inside the cell.

4) Repairing Components

It will contain DNA polymerase **(Taq) Endonuclease.**

5) Charge Receptor

It captures the electrical charges from surroundings.

6) Charge Storer

It stores the charge a certain amount of which helps to dissolve the (1) membrane.

7) Protein Gripper

8) Modified or specialised Molecules to grab the biomarkers on the surface of the Cancer cell.

9) pH Sensitive Membrane Injector (Lysosyme pipe)

In case of emergency failure of the normal mechanism it will directly administers "Lysosyme" to dissolve the cell membrane and also puts the materials of the head of the bot.

10) Lysosyme

Help to dissolve the cell membrane, in case of emergency.

11) Outer layer of the Bot

It is made up of polysaccharide, which helps the total structure to get **imbibed ([2] of References of Terminology)** by the targeted cells.

- **Steps of using or Administering the Nanobots**

1) Marking the effected cells with **Biomarkers ([1] of References of Terminology).**

2) Administering the Nanobots or Nano Capsules into the bloodstream

3) Attachment of the Engineered Nanocapsules with the effected Cancer Cells with the help of the modified molecules which react with the biomarkers, and attaches the Nanocapsules with the cells.

4) Imbibition of the NanoCapsules by the targeted Cells.

5) If natural imbibitions doesn't occure then the alternative process will be to control the pH of the surroundings of the capsules, when a particular pH value will be achieved, the Lysosyme Pipe will be dissolved and the released lysosyme will facilitate the entering of the Nanobots into the cell membrane.

6) After entering the cell the first membrane will be dissolved after acquiring electric pulse from inside the cell itself.

7) Vinblastin and Cisplatin will be released and they will stop the growth cells and start apoptosis, respectively.

8) Then, a certain value (approximate value) of the inner pH of the cell will dissolve the 2nd membrane.

9) Endonuclease and Taq polymerase will be released, and they will do their respective functions.

10) Natural degradation of the Nanobots.

References of Terminology

[1] Several protein Based Biomarkers can be used for identifying Cancer Cells like **AFP, BCR-ABL, BRCA1/BRCA2, BRAFV600E, PSA, CEA, EGFR, HER-2.**

The concept will be like this the end part of the protein molecules of the NanoBots grippers should be attachable with the biomarkers.

[2] For the imbibitions process, see the Repairing Reaction part.

REFERENCES

1. Mitchison T., Kirschner M. W. (1984) Nature, 312: 237–242. [PubMed] [Google Scholar]
2. Goldman R. D. (1971) J. Cell Biol., 51: 752–762. [PMC free article] [PubMed] [Google Scholar]
3. Small J. V., Geiger B., Kaverina I., Bershadsky A. (2002) Nat. Rev. Mol. Cell Biol., 3: 957–964. [PubMed] [Google Scholar]
4. Jordan M. A., Wilson L. (2004) Nature Reviews, 4: 253–265. [PubMed] [Google Scholar]
5. Pourroy B., Honoré S., Pasquier E., Bourgarel-Rey V., Kruczynski A., Briand C., Braguer D. (2006) Cancer Res., 66: 3256–3263. [PubMed] [Google Scholar]
6. Schwartz E. L. (2009) Clin. Cancer Res., 15: 2594–2601. [PMC free article] [PubMed] [Google Scholar]
7. Hari M., Wang Y., Veeraraghavan S., Cabral F. (2003) Mol. Cancer Ther. 2: 597–605. [PubMed] [Google Scholar]
8. Schibler M. J., Cabral F. (1986) J. Cell Biol., 102: 1522–1531. [PMC free article] [PubMed] [Google Scholar]
9. Cabral F., Sobel M. E., Gottesman M. M. (1980) Cell, 20: 29–36. [PubMed] [Google Scholar]
10. Yang H., Cabral F. (2007) J. Biol. Chem., 282: 27058–27066. [PubMed] [Google Scholar]
11. Olson K. R., McIntosh J. R., Olmsted J. B. (1995) J. Cell Biol., 130: 639–650. [PMC free article] [PubMed] [Google Scholar]
12. Minotti A. M., Barlow S. B., Cabral F. (1991) J. Biol. Chem., 266: 3987–3994. [PubMed] [Google Scholar]
13. Abraham I., Marcus M., Cabral F., Gottesman M. M. (1983) J. Cell Biol., 97: 1055–1061. [PMC free article] [PubMed] [Google Scholar]
14. Cabral F., Barlow S. B. (1991) Pharmacol. Ther., 52: 159–171. [PubMed] [Google Scholar]
15. Kung A. L., Sherwood S. W., Schimke R. T. (1990) Proc. Natl. Acad. Sci. U.S.A., 87: 9553–9557. [PMC free article] [PubMed] [Google Scholar]
16. Barlow S., Gonzalez-Garay M. L., West R. R., Olmsted J. B., Cabral F. (1994) J. Cell Biol., 126:

1017–1029. [PMC free article] [PubMed] [Google Scholar]

17. Wang X. M., Peloquin J. G., Zhai Y., Bulinski J. C., Borisy G. G. (1996) J. Cell Biol., 132: 345–357. [PMC free article] [PubMed] [Google Scholar]

18. Kamath K., Wilson L., Cabral F., Jordan M. A. (2005) J. Biol. Chem., 280: 12902–12907. [PubMed] [Google Scholar]

19. Rhoads D. S., Guan J. L. (2007) Exp. Cell Res. 313, 3859–3867. [PMC free article] [PubMed] [Google Scholar]

20. Cabral F. (2000) Drug Resist. Updat., 3: 1–6. [Google Scholar]

21. Keating T. J., Peloquin J. G., Rodionov V. I., Momcilovic D., Borisy G. G. (1997) Proc. Natl. Acad. Sci. U.S.A., 94: 5078–5083. [PMC free article] [PubMed] [Google Scholar]

22. Rusan N. M., Fagerstrom C. J., Yvon A. M., Wadsworth P. (2001) Mol. Biol. Cell, 12: 971–980. [PMC free article] [PubMed] [Google Scholar]

23. Liao G., Nagasaki T., Gundersen G. G. (1995) J. Cell Sci., 108: 3473–3483. [PubMed] [Google Scholar]

24. Vacca A., Iurlaro M., Ribatti D., Minischetti M., Nico B., Ria R., Pellegrino A., Dammacco F. (1999) Blood, 94: 4143–4155. [PubMed] [Google Scholar]

25. Hotchkiss K. A., Ashton A. W., Mahmood R., Russell R. G., Sparano J. A., Schwartz E. L. (2002) Mol. Cancer Ther., 1: 1191–1200. [PubMed] [Google Scholar]

26. Yin S., Bhattacharya R., Cabral F. (2010) Mol. Cancer Ther., 9: 327–335. [PMC free article] [PubMed] [Google Scholar]

27. Cabral F. R. (1983) J. Cell Biol., 97: 22–29. [PMC free article] [PubMed] [Google Scholar]

28. Pasquier E., Honore S., Pourroy B., Jordan M. A., Lehmann M., Briand C., Braguer D. (2005) Cancer Res., 65: 2433–2440. [PubMed] [Google Scholar]

29. Brangwynne C. P., MacKintosh F. C., Kumar S., Geisse N. A., Talbot J., Mahadevan L., Parker K. K., Ingber D. E., Weitz D. A. (2006) J. Cell Biol., 173: 733–741. [PMC free article] [PubMed] [Google Scholar]

30. Cheng G., Zile M. R., Takahashi M., Baicu C. F., Bonnema D. D., Cabral F., Menick D. R., Cooper G., 4th (2008) Am. J. Physiol. Heart Circ. Physiol, 294: H2231–H2241. [PubMed] [Google Scholar]

31. Salaycik K. J., Fagerstrom C. J., Murthy K., Tulu U. S., Wadsworth P. (2005) J. Cell Sci., 118: 4113–4122. [PubMed] [Google Scholar]

32. Abal M., Piel M., Bouckson-Castaing V., Mogensen M., Sibarita J. B., Bornens M. (2002) J. Cell Biol., 159: 731–737. [PMC free article] [PubMed] [Google Scholar]

33. Ahmad F. J., Baas P. W. (1995) J. Cell Sci., 108: 2761–2769. [PubMed] [Google Scholar]

34. Tassin A. M., Maro B., Bornens M. (1985) J. Cell Biol., 100: 35–46. [PMC free article] [PubMed] [Google Scholar]

35. Bacallao R., Antony C., Dotti C., Karsenti E., Stelzer E. H., Simons K. (1989) J. Cell Biol., 109: 2817–2832. [PMC free article] [PubMed] [Google Scholar]

36. Waterman-Storer C. M., Salmon E. D. (1997) J. Cell Biol., 139: 417–434. [PMC free article] [PubMed] [Google Scholar]

37. Rusan N. M., Wadsworth P. (2005) J. Cell Biol., 168: 21–28. [PMC free article] [PubMed] [Google Scholar]

38. Saxton W. M., Stemple D. L., Leslie R. J., Salmon E. D., Zavortink M., McIntosh J. R. (1984) J. Cell Biol., 99: 2175–2186. [PMC free article] [PubMed] [Google Scholar]

39. Mastronarde D. N., McDonald K. L., Ding R., McIntosh J. R. (1993) J. Cell Biol., 123: 1475–1489. [PMC free article] [PubMed] [Google Scholar]

40. Tulu U. S., Rusan N. M., Wadsworth P. (2003) Curr. Biol., 13: 1894–1899. [PubMed] [Google Scholar]

41. Burbank K. S., Groen A. C., Perlman Z. E., Fisher D. S., Mitchison T. J. (2006) J. Cell Biol., 175: 369–375. [PMC free article] [PubMed] [Google Scholar]

42. Srayko M., O'toole E. T., Hyman A. A., Müller-Reichert T. (2006) Curr. Biol., 16: 1944–1949. [PubMed] [Google Scholar]

43. Yang G., Houghtaling B. R., Gaetz J., Liu J. Z., Danuser G., Kapoor T. M. (2007) Nat. Cell Biol., 9: 1233–1242. [PubMed] [Google Scholar]

44. "Vinblastine Sulfate". The American Society of Health-System Pharmacists. Archived from the original on 2015-01-02. Retrieved Jan 2, 2015.

45. Ravina E (2011). The evolution of drug discovery: from traditional medicines to modern drugs (1. Aufl. ed.). Weinheim: Wiley-VCH. p. 157. ISBN 9783527326693. Archived from the original on 2017-08-01.

46. World Health Organization (2019). World Health Organization model list of essential medicines: 21st list 2019. Geneva: World Health Organization. hdl:10665/325771. WHO/MVP/EMP/IAU/2019.06. License: CC BY-NC-SA 3.0 IGO.

47. "Vinblastine". Retrieved 28 November 2015.

48. British national formulary: BNF 69 (69 ed.). British Medical Association, 2015; 593. ISBN 9780857111562.

49. Liljefors T, Krogsgaard-Larsen P, Madsen U (2002). Textbook of Drug Design and Discovery (Third ed.). CRC Press. p. 550. ISBN 9780415282888. Archived from the original on 2016-12-20.

50. "Vinblastine sulfate- vinblastine sulfate injection". DailyMed. 31 December 2019. Retrieved 15 April 2020.

51. van Der Heijden R, Jacobs DI, Snoeijer W, Hallard D, Verpoorte R (March 2004). "The Catharanthus alkaloids: pharmacognosy and biotechnology". Current Medicinal Chemistry, 11(5): 607–28. doi:10.2174/0929867043455846. PMID 15032608.

52. Cooper R, Deakin JJ (2016). "Africa's gift to the world". Botanical Miracles: Chemistry of Plants

That Changed the World. CRC Press, 46–51. ISBN 9781498704304. Archived from the original on 2017-08-01.

53. Keglevich P, Hazai L, Kalaus G, Szántay C (May 2012). "Modifications on the basic skeletons of vinblastine and vincristine". Molecules, 17(5): 5893–914. doi:10.3390/molecules17055893. PMC 6268133. PMID 22609781.

54. Sears JE, Boger DL (March 2015). "Total synthesis of vinblastine, related natural products, and key analogues and development of inspired methodology suitable for the systematic study of their structure-function properties". Accounts of Chemical Research, 48(3): 653–62. doi:10.1021/ar500400w. PMC 4363169. PMID 25586069.

55. Altmann K (2009). "Preclinical Pharmacology and Structure-Activity Studies of Epothilones". In Mulzer JH (ed.). The Epothilones: An Outstanding Family of Anti-Tumor Agents: From Soil to the Clinic. Springer Science & Business Media, 157–220. ISBN 9783211782071. Archived from the original on 2017-09-11.

56. Starling D (January 1976). "Two ultrastructurally distinct tubulin paracrystals induced in sea-urchin eggs by vinblastine sulphate" (PDF). Journal of Cell Science, 20(1): 79–89. PMID 942954. Archived (PDF) from the original on 2014-01-13.

57. Gobbi PG, Broglia C, Merli F, Dell'Olio M, Stelitano C, Iannitto E, et al. (December 2003). "Vinblastine, bleomycin, and methotrexate chemotherapy plus irradiation for patients with early-stage, favorable Hodgkin lymphoma: the experience of the Gruppo Italiano Studio Linfomi". Cancer, 98(11): 2393–401. doi:10.1002/cncr.11807. hdl:11380/4847. PMID 14635074.

58. Jordan MA, Wilson L (April 2004). "Microtubules as a target for anticancer drugs". Nature Reviews. Cancer, 4(4): 253–65. doi:10.1038/nrc1317. PMID 15057285.

59. Yang H, Ganguly A, Cabral F (October 2010). "Inhibition of cell migration and cell division correlates with distinct effects of microtubule inhibiting drugs". The Journal of Biological Chemistry, 285(42): 32242–50. doi:10.1074/jbc.M110.160820. PMC 2952225. PMID 20696757.

60. Kuehne ME, Matson PA, Bornmann WG (1991). "Enantioselective Syntheses of Vinblastine, Leurosidine, Vincovaline, and 20'-epi-Vincovaline". Journal of Organic Chemistry, 56(2): 513–528. doi:10.1021/jo00002a008.

61. Yokoshima S, Tokuyama H, Fukuyama T (2009). "Total Synthesis of (+)-Vinblastine: Control of the Stereochemistry at C18″". The Chemical Record, 10(2): 101–118. doi:10.1002/tcr.200900025.

62. Noble RL, Beer CT, Cutts JH (December 1958). "Role of chance observations in chemotherapy: Vinca rosea". Annals of the New York Academy of Sciences, 76(3): 882–94. doi:10.1111/j.1749-6632.1958.tb54906.x. PMID 13627916.

63. Chen CC, Hsiao FY, Shen LJ, Wu CC. The cost-saving effect and prevention of medication errors by clinical pharmacist intervention in a nephrology unit. Medicine (Baltimore), 2017 Aug; 96(34): e7883. [PMC free article] [PubMed]

64. Di Muzio M, Tartaglini D, De Vito C, La Torre G. Validation of a questionnaire for ICU nurses to assess knowledge, attitudes and behaviours towards medication errors. Ann Ig., 2016 Mar-Apr; 28(2): 113-21. [PubMed]

65. Cohen, J. D. et al. Detection and localization of surgically resectable cancers with a multi-analyte blood test. Science https://doi.org/10.1126/science.aar3247 (2018)

66. Genetic pathways and mutation profiles of human cancers: site- and exposure-specific patterns. I.A. Lea, M.A. Jackson, X. Li, S. Bailey, S.D. Peddada, and J.K. Dunnick.

67. Pathway Based Analysis of Mutation Data Is Efficient for Scoring Target Cancer Drugs Marianna A. Zolotovskaia, Maxim I. Sorokin, Anna A. Emelianova, Nikolay M. Borisov, Denis V. Kuzmin, Pieter Borger, Andrew V. Garazha, and Anton A. Buzdin.

68. Schwappach DLB, Taxis K, Pfeiffer Y. Oncology nurses' beliefs and attitudes towards the double-check of chemotherapy medications: a cross-sectional survey study. BMC Health Serv Res., 2018 Feb 17; 18(1): 123. [PMC free article] [PubMed]

69. CancerSEEK and destroy — a blood test for early cancer detection David Killock in *Nature Reviews Clinical Oncology,* 2018; 15: page133.

Conversion Table
• 1 kilogram (kg) = 1000 grams (g) • 1 gram (g) = 1000 milligrams (mg) – Convert Grams to Milligrams by Multiplying grams by 1,000 – Convert Milligrams to grams by dividing milligrams by 1,000 • 1 milligram (mg) = 1000 micrograms (mcg) • Grains (gr.) 15 = 1 Gram (g) or 1000 milligrams (mg) – To convert g. to gr multiply by 15 – To convert gr to g divide by 15. • 1 Grain (gr.) = 60 Milligrams (mg) – To convert gr. to mg multiply gr. by 60 – To convert mg to gr. divide mg. by 60 • 1ml = 1 cc • 1 ounce = 30 ml • 1 tablespoon (T or tbsp) = 15 ml • 1 teaspoon (t or tsp) = 5 ml • 2.2 lb = 1 kg • To convert pounds to kg divide pounds by 2.2 • To convert kg to pounds multiply by 2.2